ACS BIO & MED CHEM Au
AN OPEN ACCESS JOURNAL OF THE AMERICAN CHEMICAL SOCIETY

pubs.acs.org/biomedchemau
Article

A Bioluminescent Probe for H_2S Detection in Tumor Microenvironment

Published as part of ACS Bio & Med Chem Au special issue "2024 Rising Stars in Biological, Medicinal, and Pharmaceutical Chemistry".

Kang Lu,[⊥] Yixian Wang,[⊥] Chenhang Wang, Rui Liu, Kaiqiang Yang, Xuanchenye Zhang, and Han Xiao*

Cite This: ACS Bio Med Chem Au 2025, 5, 175−183
Read Online

ACCESS | Metrics & More | Article Recommendations | Supporting Information

ABSTRACT: Hydrogen sulfide (H_2S) is an endogenous gaseous signaling molecule that regulates various physiological functions, and its abnormal levels have been closely linked to the onset and progression of numerous diseases including renal cell carcinoma (RCC). RCC is the most common malignant tumor of the kidney, accounting for 85−90% of all kidney cancer cases. However, studies using H_2S as a biomarker for monitoring RCC progression at the molecular level remain relatively limited. Most current H_2S luminescent probes suffer from low sensitivity and often need external stimuli, such as cysteine, to artificially elevate H_2S levels, thereby reducing their effectiveness in detecting H_2S in cells or in vivo. Although bioluminescent imaging probes are gaining attention for their specificity and high signal-to-noise ratio, no existing probes are specifically designed for detecting H_2S in RCC. Additionally, many bioluminescent probes face challenges such as short emission wavelengths or dependence on complex conditions such as external adenosine triphosphate (ATP). Herein, through "caging" the luciferin substrate QTZ with H_2S recognition groups, a H_2S-sensitive bioluminescent probe QTZ-N_3 with good sensitivity (~0.19 μM) and selectivity was prepared. QTZ-N_3 can effectively detect endogenous H_2S in 786-O-Nluc renal cancer cells and sensitively monitor H_2S levels in the RCC xenograft nude mouse model without requiring stimuli like cysteine. Furthermore, QTZ-N_3 allows for the real-time monitoring of H_2S during tumor progression. This work lays a solid foundation for future understanding of the biological functions of H_2S in vivo.

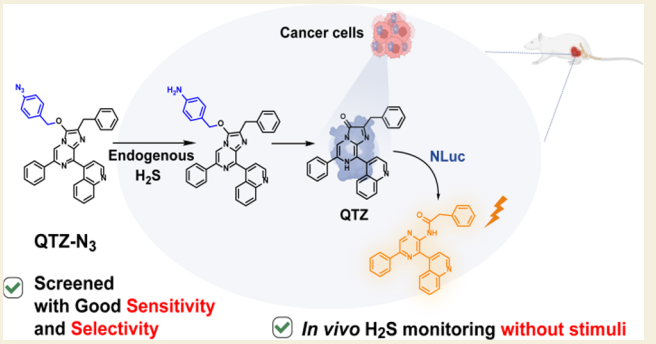

KEYWORDS: *hydrogen sulfide (H_2S), renal cell carcinoma (RCC), bioluminescence, bioluminescent imaging, biological imaging, tumor microenvironment, luciferase*

INTRODUCTION

Hydrogen sulfide (H_2S), a renowned messaging transmitter, is endogenously generated from cysteine (Cys)-related substrates by enzymes including cystathionine-γ-lyase (CSE), cystathionine-β-synthase (CBS), and 3-mercaptopyruvate sulfur transferase (3-MST)/cysteine aminotransferase (CAT).[1,2] H_2S is a lipophilic molecule that can permeate cell membranes without transporters and acts as a signaling messenger in regulating vital processes.[3] Homeostasis of H_2S is involved in cell protection pathways, such as antioxidant, antiapoptosis, and anti-inflammation.[4−7] Nevertheless, uncontrolled production of H_2S, especially in renal cell carcinoma (RCC), can regulate inflammatory responses, oxidative stress, and mitochondrial dysfunction, ultimately leading to kidney injury and fibrosis.[8,9] RCC, which accounts for 85−90% of adult renal malignancies, is the most common form of kidney cancer.[10,11] Despite its prevalence, the molecular biology of RCC remains complex and poorly understood, with many signaling pathways yet to be identified.[12,13] Considering the significance of H_2S in biological systems, particularly in RCC, the development of a tool to detect H_2S in RCC for molecular biological research is highly desirable.

Currently, several methods for detecting H_2S exist, including colorimetric,[14] gas chromatography,[15] electrochemical,[16] and voltammetric methods.[17] However, these methods have inherent drawbacks such as poor compatibility with live cells due to postmortem tissue or cell lysate damage, making real-time in vivo H_2S detection challenging. Furthermore, small-molecule fluorescent probes face limitations in biological

Received: September 27, 2024
Revised: December 19, 2024
Accepted: December 20, 2024
Published: January 3, 2025

https://doi.org/10.1021/acsbiomedchemau.4c00102
ACS Bio Med Chem Au 2025, 5, 175−183

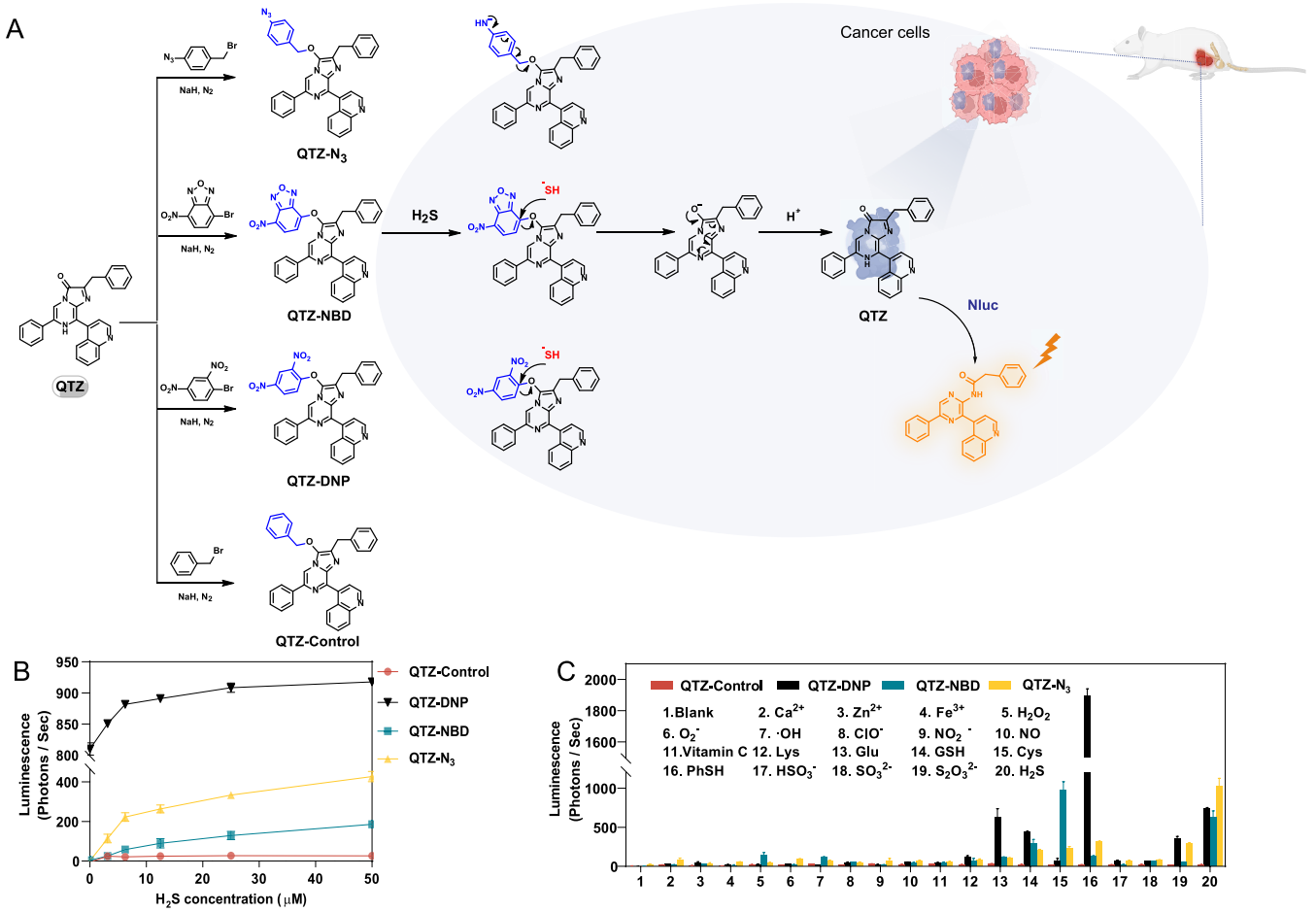

Figure 1. (A) Synthetic route and screening of the bioluminescent H_2S probes (QTZ-N_3, QTZ-DNP, QTZ-NBD) and QTZ-Control; (B) Comparison of the luminescent reactivities of four compounds (QTZ-Control, QTZ-DNP, QTZ-NBD, and QTZ-N_3) (100 μM) with different concentrations of NaSH and 0.5 μg/mL Nluc in PBS buffer (pH 7.4, 10 mM) after incubation at 37 °C for 30 min; (C) Bioluminescence responses of four compounds (QTZ-Control, QTZ-DNP, QTZ-NBD, and QTZ-N_3) (100 μM) toward different analytes in PBS buffer (pH 7.4, 10 mM) after incubation at 37 °C for 30 min: blank (1), 100 μM metal ions (2−4: Ca^{2+}, Zn^{2+}, and Fe^{3+}), 100 μM RONS (5−10: H_2O_2, O_2^-, •OH, ClO^-, NO_2^-, NO), 1 mM biological reductants (11−15: vitamin C, Lys, Glu, GSH, Cys), 1 mM reactive sulfur species (16−19: PhSH, HSO_3^-, SO_3^{2-}, and $S_2O_3^{2-}$), and 500 μM H_2S (20). Data are presented as mean ± SD (n = 3).

applications due to autofluorescence and poor tissue penetration.[18−20] These probes also tend to lack the sensitivity needed to detect low H_2S levels typically found in biological systems.[21] Previous H_2S probes were only capable of detecting high H_2S concentrations in mouse models induced by stimuli such as lipopolysaccharides or cysteine. This limitation restricts their utility for studying H_2S under physiological conditions in vivo.[22−25] In contrast, bioluminescence, produced by the reaction of luciferin with luciferase, offers high signal-to-noise ratios and can be genetically encoded to target specific cells or tissues, providing more sensitive and specific detection.[26−28] Scientists use "caging" chemical modifications to temporarily block luciferase−luciferin reactions, which restore upon encountering specific analytes (enzymes,[29] and some chemicals[30−32]), and then generate bioluminescence. Firefly luciferin has been "caged" with aryl azide or 2,4-dinitrophenyl (DNP) for the detection of H_2S in cells and mice.[33−35] However, the inherent adenosine triphosphate (ATP) dependence of the firefly luciferase−luciferin system limits its applicability in cellular applications. In contrast, marine luciferases, like Renilla luciferase, do not rely on ATP, making them more suitable for imaging analysis in biological systems.[36] Recently, researchers have developed marine luciferase variants with higher catalytic activity and stability, such as NanoLuc luciferase (Nluc)−furimazine (FRZ). Despite progress, the short-wavelength blue emission (~450 nm) of the Nluc−FRZ pair limits its widespread application for in vivo studies. To achieve a red-shift of Nluc emissions into the in vivo optical imaging window (600−950 nm), researchers are exploring various strategies, including the chemical modification of FRZ to form QTZ.[37] The QTZ luciferin and paired Nluc variant exhibit bright bioluminescence with a peak emission at ~585 nm. The Nluc-QTZ system offers advantages of ATP independence, high stability, and red-shifted emission, enabling tumor imaging in xenograft mouse models.[37]

Herein, we report the design, synthesis, and evaluation of a H_2S-sensitive bioluminescent probe with good sensitivity and selectivity for monitoring H_2S levels at the physiological level in vivo. Specifically, we designed H_2S-responsive probes using three "caged" groups: DNP, 7-nitrobenzofurazan (NBD), and benzyl azide. In the presence of H_2S, these "caged" luciferins undergo a self-cleavage process and generate QTZ, which can be catalyzed by Nluc to produce bioluminescence. Through sensitivity and selectivity screening, we demonstrated that QTZ-N_3 exhibits the best capability to selectively detect H_2S over other biologically relevant reactive sulfur species (RSS).

https://doi.org/10.1021/acsbiomedchemau.4c00102
ACS Bio Med Chem Au 2025, 5, 175−183

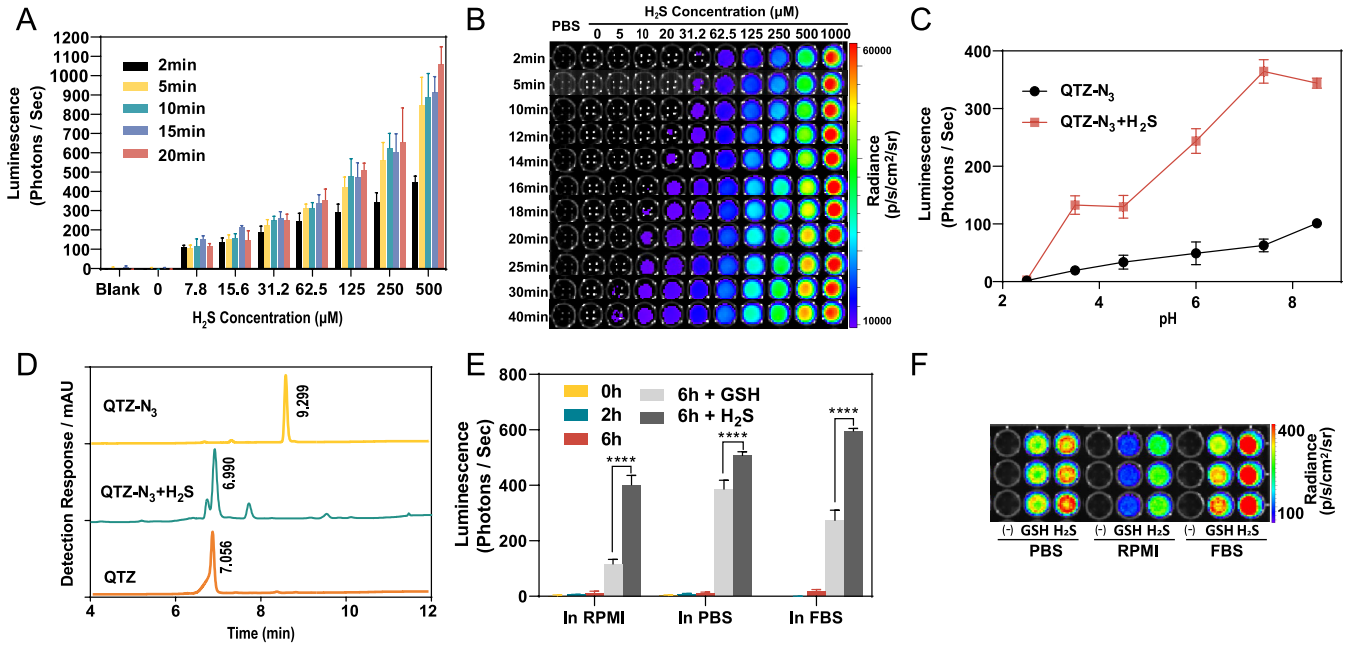

Figure 2. (A) Bioluminescent response of QTZ-N_3 (100 μM) when treated with increased NaSH concentrations and Nluc (0.5 μg/mL) in PBS buffer (10 mM, pH 7.4) for different incubation times at 37 °C. (B) Representative bioluminescence images of (A) shown in 96-well black plates. (C) Bioluminescent signal of QTZ-N_3 (50 μM) in the absence and presence of NaSH (20 μM) and 0.5 μg/mL Nluc over a wide pH range. (D) High-performance liquid chromatography (HPLC) traces of the incubation mixture of QTZ-N_3 (100 μM) in the absence (upper panel) or presence (middle panel) of NaSH (200 μM) in PBS buffer (pH 7.4, 10 mM) for 5 min at 37 °C and HPLC traces of QTZ (60 μM) (lower panel) in PBS buffer (pH 7.4, 10 mM). Wavelength: 254 nm. (E) Stability test of QTZ-N_3 in PBS buffer (pH 7.4), cell culture medium RPMI 1640, and fetal bovine serum (FBS), as well as the luminescence response test with GSH (10 mM) and NaSH (100 uM). (F) Representative bioluminescence images of figure (E) are shown in 96-well black plates. Data are presented as mean ± SD (n = 3).

We further evaluated the utility of this probe in monitoring changes in H_2S levels in RCC cells as well as living animals (Figure 1A).

RESULTS AND DISCUSSION

Design and Characterization of Bioluminescent H_2S Probes

In 2022, Ai and co-workers reported the discovery of QTZ for molecular imaging of tumor-associated antigens.[37] QTZ offers several advantages: (1) extended conjugations in the imidazopyrazinone core cause red-shifted bioluminescence when paired with Nluc, resulting in improved performance for imaging deep-tissue targets in living mice; and (2) with a molecular weight of only 19 kDa, the constructed QTZ-Nluc system demonstrates high physical stability and good reactivity.[38] Despite the above advantages, researchers are developing new QTZ-based platforms that can respond to specific analytes, thereby expanding their biological application. One common approach is the "caging" of luciferins, where chemically protective groups are introduced at the enolized keto position on the C-3 carbon of the imidazopyrazinone core to stabilize the luciferin.[39] Consequently, various bioluminescent probes have been developed using this caged luciferin strategy, and when these protective groups are cleaved by specific targets, such as enzymes or biomolecules, the caged luciferin is converted into its free form, thereby emitting bioluminescence.[39−41] To develop a H_2S-responsive bioluminescent probe for the QTZ-Nluc system, we modified QTZ by attaching H_2S recognition groups, which are expected to react specifically with H_2S, thus triggering an electron cascade that reveals the parent QTZ. The synthesis of QTZ began with 5-bromo-3-iodopyrazin-2-amine, which underwent two Suzuki coupling steps to form the key pyrazine core (5-phenyl-3-(quinolin-4-yl) pyrazin-2-amine), and this pyrazine core was then condensed with a diethoxy derivative in ethanol and concentrated HCl to generate QTZ. In our H_2S-responsive bioluminescent probes, we selected three H_2S recognition sites based on thiolysis or azide reduction mechanisms, including DNP, NBD, and benzyl azide.[42−45] QTZ underwent nucleophilic substitution with the halogen atoms of these recognition groups to produce the target compounds QTZ-DNP, QTZ-NBD, and QTZ-N_3 (Figure 1A). To verify the effectiveness of the recognition groups and their "caging" ability on the luciferin QTZ, we synthesized a control compound, QTZ-Control, using benzyl bromide (Figure 1A). Detailed synthesis steps and characterization are provided in the Supporting Information.

Reactivity and Selectivity Screening of Bioluminescent H_2S Probes toward H_2S

With four candidates in hand, we first evaluated the reactivities of these compounds toward H_2S under physiological conditions (Figure 1B). Since H_2S concentrations in cells are estimated to be in the nanomolar to low micromolar range, examining the sensitivity of the probe is crucial.[46] NaSH was used as the H_2S donor in our experiments, given its similar ion distribution to H_2S in physiological aqueous solutions.[47] Under physiological pH, H_2S predominantly exists as HS^-. We performed both time- and concentration-response analyses. QTZ-DNP exhibited stronger luminescence signals with increasing H_2S concentration and a rapid response within 15 min (Figure S2A). However, QTZ-DNP emitted a high luminescence (~800 photons/seconds) in phosphate-buffered

https://doi.org/10.1021/acsbiomedchemau.4c00102
ACS Bio Med Chem Au 2025, 5, 175−183

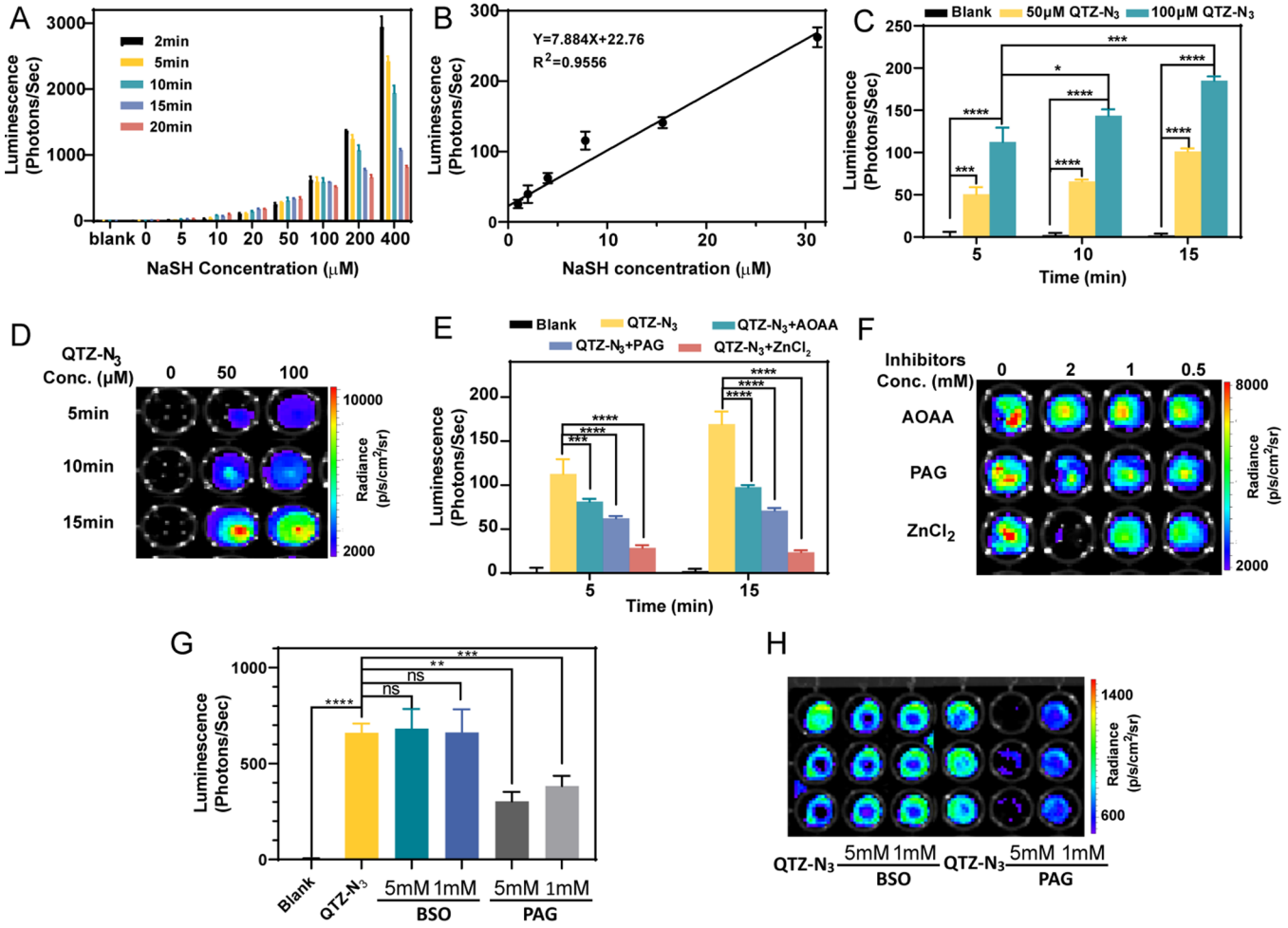

Figure 3. (A) Exogenous H_2S bioluminescent response of QTZ-N_3 (100 μM) when treated with increased NaSH concentrations in 786-O-Nluc cells for different incubation times at 37 °C. (B) Concentration-dependent luminescence changes after an incubation time of 5 min. The linear relationship is described as $y = 7.884x + 22.76$ ($R^2 = 0.9556$), and the linearity range of H_2S is from 0.54 to 30 μM. (C) Bioluminescent response of endogenous H_2S in 786-O-Nluc cells toward different concentrations of QTZ-N_3 (0, 50, and 100 μM) for different incubation times (5, 10, and 15 min), respectively, at 37 °C. (D) Representative bioluminescence images of figure (C) are shown in 96-well black plates. (E) Inhibitory effect of QTZ-N_3 on endogenous H_2S production in 786-O-Nluc cells at different times (5 and 15 min). Groups: 786-O-Nluc cells only treated with 100 μM QTZ-N_3 for 30 min at 37 °C; pretreated with 2, 1, or 0.5 mM AOAA, PAG, or $ZnCl_2$ for 2 h, followed by incubation with 100 μM QTZ-N_3 for 30 min at 37 °C. (F) Representative bioluminescence images of figure (E) are shown in 96-well black plates at 15 min. (G) Comparison of inhibitory effects of PAG (5 or 1 mM) on endogenous H_2S and BSO (5 or 1 mM) on endogenous GSH in 786-O-Nluc cells incubated with QTZ-N_3. (H) Representative bioluminescence images of figure (G) are shown in 96-well black plates. Data are presented as mean ± SD ($n = 3$). P values were determined by one-way ANOVA with Tukey's multiple comparisons test. *$P < 0.05$, **$P < 0.01$, ***$P < 0.001$, ****$P < 0.0001$.

saline (PBS) (pH 7.4, 10 mM) even in the absence of NaSH. This suggested that QTZ-DNP is relatively unstable under mild conditions, prone to decomposition, and can generate false-positive signals, which limits the accurate detection of H_2S in biological systems. For the other three compounds, compared to QTZ-NBD, QTZ-N_3 provided a stronger luminescent signal, demonstrating good concentration-dependent enhancement (0−50 μM) (Figures 1B, 2A,B, and S2B) and time-dependent increase (30 min) (Figures 2A, 2B, and S2B). The limit of detection of QTZ-N_3 toward H_2S in an aqueous solution is 0.19 μM (Figure S4). In contrast, the QTZ-control did not react with H_2S and exhibited nondetectable luminescent signal (Figure 1B).

Due to the diversity of interfering ions in biological research, the selectivity of H_2S probes is a crucial parameter. More importantly, some SH^- containing biomolecules, such as glutathione (GSH) and Cys, may participate in the thiolysis of DNP, NBD, and azide reduction, reducing the selectivity of the probe.[42] Therefore, to detect the selectivities of QTZ-DNP, QTZ-NBD, and QTZ-N_3, probes were incubated in PBS (pH 7.4, 10 mM) with millimolar levels of GSH, Cys, and Glu, as well as micromolar levels of H_2S. In addition, thiophenol was tested as well since its overproduction can lead to various diseases such as central nervous system damage, coma, and even death.[48,49] The results indicated that QTZ-DNP was more affected by thiophenol and Glu, and its reactivity toward thiophenol was ∼1.8 times higher than that of H_2S (Figure 1C). This might be due to the strong electron-withdrawing DNP ethers being prone to thiolysis. QTZ-NBD demonstrated a higher reactivity toward Cys than H_2S (Figure 1C), which is due to the fact that H_2S and thiols readily undergo nucleophilic aromatic substitution with electrophilic NBD derivatives to produce NBD-SH and NBD-SR compounds.[50] In contrast, QTZ-N_3 showed better selectivity for H_2S over multiple RSS (Figures 1C and S3). The good selectivity is likely due to the different pK_a values of H_2S, Cys, and GSH at physiological pH

https://doi.org/10.1021/acsbiomedchemau.4c00102
ACS Bio Med Chem Au 2025, 5, 175−183

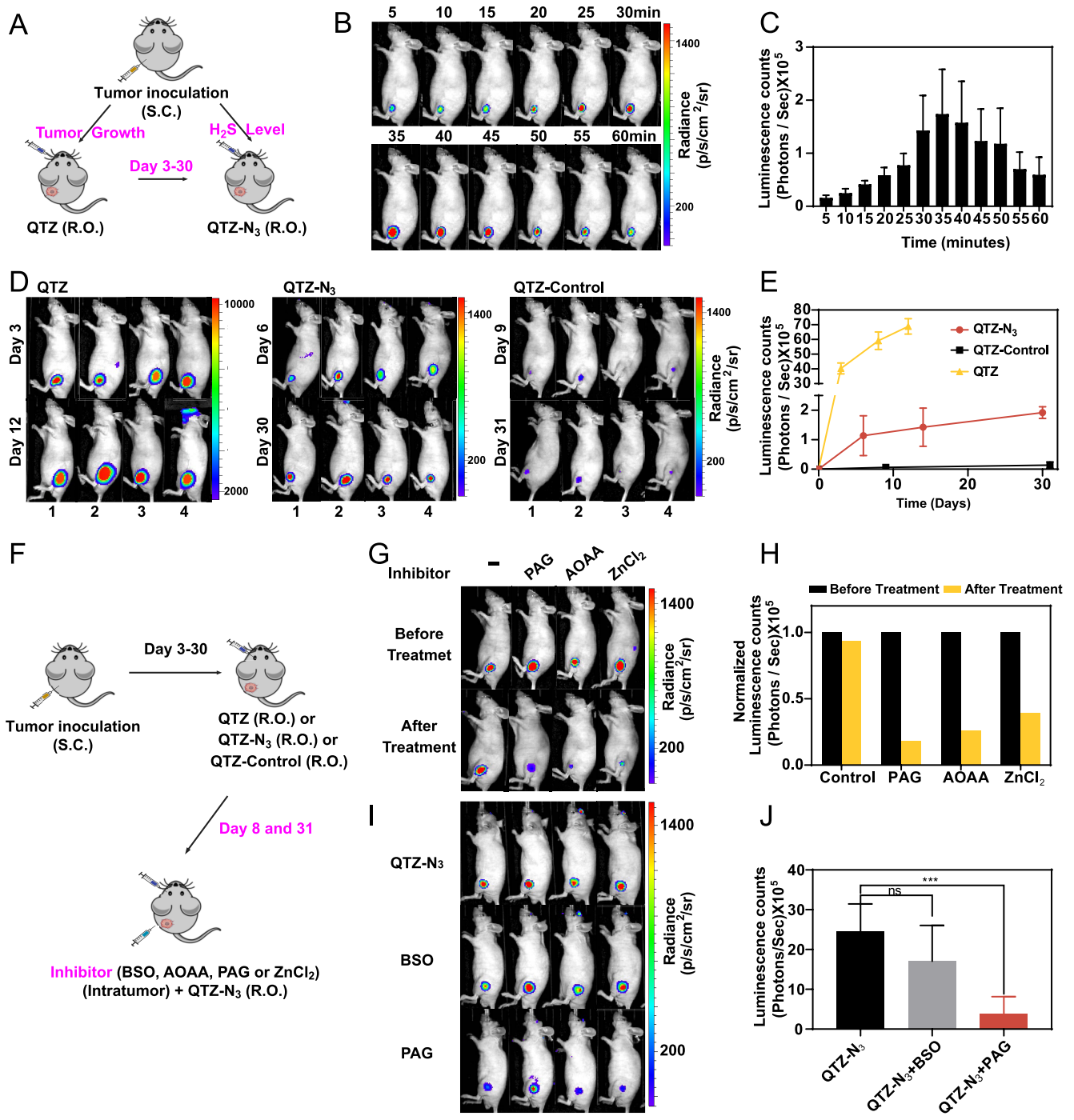

Figure 4. (A) Schematic illustration of the 786-O-Nluc xenograft tumor mouse model using QTZ and QTZ-N_3; (B) Bioluminescence imaging of endogenous H_2S in 786-O-Nluc xenograft tumor-bearing mice. The mice were intravenously injected with QTZ-N_3 (100 μL, 1 mM). (C) Relative bioluminescence intensity in figure (A). (D) Tumor growth monitored using the luciferin substrate QTZ (100 μL, 1 mM) on days 3 and 12. Fluctuations of H_2S in the tumor monitored using QTZ-N_3 (100 μL, 1 mM) on days 6 and 30 and with QTZ-Control (100 μL, 1 mM) on days 9 and 31 in 786-O-Nluc xenograft tumor-bearing mice. (E) Relative bioluminescence intensity of three groups in figure (D) and Figure S10. (F) Schematic illustration of the 786-O-Nluc xenograft tumor mouse model using inhibitors. (G) Bioluminescence imaging of endogenous H_2S in 786-O-Nluc xenograft tumor-bearing mice. Mice in the control group were intravenously injected with QTZ-N_3 (100 μL, 1 mM), while mice in the inhibitor groups were intratumorally injected with PAG, AOAA, or $ZnCl_2$ (50 μL, 2 mM) and then intravenously injected with QTZ-N_3 (100 μL, 1 mM). (H) Relative bioluminescence intensity in (G). (I) Inhibitory effects of PAG (5 and 1 mM) and BSO (5 and 1 mM) in 786-O-Nluc xenograft tumor-bearing mice. Mice in the control group were intravenously injected with QTZ-N_3 (100 μL, 1 mM), while mice in the inhibitor groups were intratumorally injected with PAG or BSO (50 μL, 2 mM) and then intravenously injected with QTZ-N_3 (100 μL, 1 mM). (J) Bioluminescence intensity in figure (I). Data are presented as mean ± SD (n = 4). P values were determined by one-way ANOVA with Tukey's multiple comparisons test. ***P < 0.001.

(Figure S1). Other substances tested, such as amino acids (Lysine), vitamin C, reactive oxygen species (H_2O_2, etc.), various anions, and metal ions, had negligible effects on QTZ-N_3. We also found that QTZ-Control had almost no reactivity

https://doi.org/10.1021/acsbiomedchemau.4c00102
ACS Bio Med Chem Au 2025, 5, 175−183

toward H_2S and other species (Figure 1C), indicating the designed H_2S recognition groups are effective for H_2S detection. Thus, QTZ-N_3 was chosen for H_2S detection in further studies due to its good stability, sensitivity, and selectivity.

Bioluminescence Imaging of QTZ-N_3 toward H_2S In Vitro

To further determine QTZ-N_3's performance, we conducted a study of QTZ-$N_3$with H_2S in PBS buffer (pH 7.4, 10 mM). The time- and concentration-dependent luminescence spectra (Figure 2A,B) revealed that QTZ-N_3 (100 μM) exhibited a strong response to H_2S under 0.5 μg/mL Nluc in PBS buffer. Moreover, the addition of 5.0 equiv of NaSH induced a rapid luminescence response within 20 min, with an emission wavelength of 467 nm (Figure S5). We also explored the pH stability of QTZ-N_3 (Figure 2C), observing that the optimal response occurred at physiological pH (7.4). Next, we verified the mechanism by which H_2S triggers the release of QTZ from QTZ-N_3 (Figures 2D and S6). The reaction products were recorded using liquid chromatography−mass spectrometry (LC−MS), and the retention time of the product (6.990 min) matched closely with that of QTZ. The mass spectrum peak at 429.2 confirmed that the product was QTZ ($[M + H]^+$ calculated for $C_{28}H_{21}N_4O$: 429.17). The proposed mechanism suggests that the aromatic azide of QTZ-N_3 is reduced to an amine. This is followed by cascade reactions and rearrangement-elimination processes, resulting in the release of QTZ.[51] Subsequently, QTZ is catalyzed by Nluc, generating light (Scheme S1).[37] Furthermore, the concentration of endogenous GSH can reach up to 10 mM, while the endogenous H_2S level is estimated to be in the low μM range. To evaluate the selectivity of QTZ-N_3, its response to 10 mM GSH and 100 μM H_2S over time was measured in different media. Notably, negligible changes in luminescence intensity were observed in PBS (pH 7.4, 10 mM), RPMI 1640 cell culture medium, or FBS after 6 h of incubation, indicating the good stability of QTZ-N_3. After adding 10 mM GSH and 100 μM H_2S for 40 min, QTZ-N_3 showed better reactivity toward H_2S than GSH (Figure 2E). These results confirm that QTZ-N_3 exhibits good sensitivity, selectivity, and stability, providing a solid foundation for H_2S detection using QTZ-N_3 in cells and living organisms.

Bioluminescence Imaging of H_2S in Living Cells

Next, we evaluated the capability of QTZ-N_3 to detect the H_2S level in living cells. 786-O cells, commonly used in RCC research, were employed in this study.[52] First, we used lentivirus-mediated transduction and clonal single-cell proliferation techniques to successfully introduce Nluc into 786-O cells, creating a 786-O-Nluc cell line with a stable expression of Nluc. Detailed experiments are provided in the Supporting Information (Tables S1 and S2). Then, we studied the cytotoxicity of QTZ-N_3 in 786-O-Nluc cells. Results showed that QTZ-N_3 has a relatively low cytotoxicity with cell viability over 80% at 500 μM, indicating its good compatibility and suitability for cell imaging (Figure S7). To detect exogenous H_2S in 786-O-Nluc cells, we incubated the cells with 100 μM QTZ-N_3 and different concentrations of NaHS. Luminescence response fluctuations were measured at 2, 5, 10, 15, and 20 min. Results indicated that the bioluminescence intensity correlated with the NaHS concentration (Figure 3A), detecting H_2S as low as 0.34 μM in living cells (Figure 3B). The faster luminescence response in cells than that in PBS buffer is due to the rapid consumption of QTZ-N_3. Incubation of 50 μM QTZ-N_3 in 786-O-Nluc cells resulted in significant luminescence, likely due to endogenous H_2S produced by live cells. The bioluminescence intensity increases as the concentrations of QTZ-N_3 rise (Figure 3C,D). Similarly, longer incubation times led to a stronger luminescent signal. These results demonstrated that QTZ-N_3 had good cell permeability and capability to monitor endogenous H_2S. We also quantified the endogenous H_2S content in 786-O-Nluc using a methylene blue colorimetric assay (Table S3 and Figure S8).[33] To further examine whether endogenous H_2S triggered luminescence, we pretreated 786-O-Nluc cells with two H_2S-generating enzyme inhibitors, aminooxyacetic acid (AOAA)[53] and propargylglycine (PAG),[54] as well as the H_2S scavenger $ZnCl_2$[23]. After incubating 786-O-Nluc cells with AOAA, PAG, or $ZnCl_2$ for 30 min, QTZ-N_3 (100 μM) was added for cellular bioluminescence imaging. Compared to untreated cells, the bioluminescence of cells treated with inhibitors significantly decreased, with the signal of PAG dropping from 169.3 ± 15.6 to 71.0 ± 3.0 ($P < 0.0001$), AOAA was decreased to 97.7 ± 2.3 ($P < 0.0001$), and $ZnCl_2$ to 23.7 ± 2.7 ($P < 0.0001$) at 15 min, indicating that PAG and $ZnCl_2$ are more effective inhibitors (Figure 3E,F). Indeed, PAG is reported to be a specific CSE inhibitor, while AOAA inhibits both CSE and CBS.[55] Considering that the GSH concentration in living organisms can reach up to 10 mM, we next assessed the ability of QTZ-N_3 to specifically detect H_2S, rather than GSH, in 786-O-Nluc cells. γ-Glutamylcysteine synthetase (γ-GCS) is responsible for GSH synthesis in cells, and the γ-GCS inhibitor L-buthionine sulfoximine (BSO) is known to effectively deplete intracellular GSH.[56] To eliminate the effect of GSH, we pretreated the cells with BSO and measured the bioluminescence intensity. The results in Figure 3G,H show that BSO had no significant effect on the bioluminescence level of QTZ-N_3 in 786-O-Nluc cells, while the PAG-treated group exhibited luminescence decrease ($P < 0.01$ and $P < 0.001$). These findings suggest that QTZ-N_3 can serve as a sensitive and specific probe to identify endogenous H_2S of living cells.

Bioluminescence Imaging in 786-O-Nluc Xenograft Nude Mice

After confirming the excellent H_2S response of QTZ-N_3 in aqueous solutions and cells, we explored whether this probe could serve as a reporter for H_2S in vivo. We constructed an RCC mouse model by injecting 786-O-Nluc cells into the flank of NU/J female mice. We intravenously injected QTZ-N_3 into the tumor-bearing mice, and then the bioluminescent imaging was measured (Figure 4A). To determine the optimal imaging time, we performed bioluminescence imaging on nude mice at various intervals from 5 to 60 min (Figure 4B,C). The results showed that the luminescence intensity increased gradually, peaked at 35 min, and remained stable for about 5 min, after which the intensity began to decline due to the consumption of QTZ-N_3. Therefore, we selected 35 min as the optimal time point for subsequent imaging to ensure maximum signal intensity and image quality. Importantly, QTZ serves as an effective substrate for Nluc, allowing for the detection of tumor occurrence and progression, while QTZ-N_3 sensitively responds to H_2S levels in the tumor microenvironment. To quantify fluctuations of H_2S during tumor growth, we alternated intravenous injections of QTZ and QTZ-N_3 on different days. The results revealed that luminescent intensity from the tumors gradually increased on days 3, 8, and 12,

https://doi.org/10.1021/acsbiomedchemau.4c00102
ACS Bio Med Chem Au 2025, 5, 175−183

indicating the growth of RCC (Figures 4D,E and S10), and tumor size measurements further confirmed the successful establishment of the RCC model (Figure S9). Additionally, the signal of QTZ-N_3 also increased on days 6, 14, and 30 (Figures 4D,E and S10). These findings strongly suggest that, during renal cancer progression, QTZ-N_3 can noninvasively monitor H_2S levels in real time, highlighting its potential as a valuable tool for assessing tumor microenvironments. Notably, currently available H_2S probes often require the use of Cys as an inducer for H_2S generation,[20,22] which significantly reduces the effectiveness of these probes for in situ monitoring of H_2S at physiological conditions in vivo. As a control, 786-O-Nluc xenograft mice injected with QTZ-Control showed a weak bioluminescent background (Figure 4D,E), confirming that QTZ-N_3 is a robust tool for detecting H_2S in vivo. Furthermore, we evaluated the efficacy of H_2S-generating enzyme inhibitors in vivo (Figure 4F). We pretreated tumor sites with inhibitors (PAG and AOAA) and a scavenger ($ZnCl_2$) for 4 h. As shown in Figure 4G,H, compared to the control group, the bioluminescence inhibition ratio in PAG-pretreated mice (82.1%) was significantly lower than that observed in the AOAA (74.5%) and $ZnCl_2$ (60.9%) groups. Finally, we evaluated the specificity of QTZ-N_3 in detecting H_2S. To eliminate the impact of high GSH concentrations, we injected BSO into mice to lower the GSH levels. The results in Figure 4I,J showed that BSO treatment did not significantly affect the tumor imaging of QTZ-N_3, whereas the PAG group exhibited a significant difference ($P < 0.001$). These findings provide strong evidence of the specificity of QTZ-N_3 in detecting H_2S in vivo. Altogether, these results demonstrate that QTZ-N_3 can be used to monitor H_2S in vivo, thereby facilitating further investigation into its biological functions.

CONCLUSIONS

In summary, a H_2S sensor library, including QTZ-DNP, QTZ-NBD, and QTZ-N_3, was designed by caging a QTZ luciferin with three H_2S reactive groups. Through sensitivity and selectivity screening, QTZ-N_3 exhibits the best sensitivity of H_2S and good selectivity against various sulfur-containing reducing species. Unlike other bioluminescent probes for H_2S detection, this new Nluc-QTZ-N_3 sensing system does not require external ATP, simplifying the experimental conditions. Additionally, it can sensitively detect H_2S at physiological concentrations in both live cells and animals without requiring stimuli like Cys. Considering the critical role of H_2S as a signaling molecule in cancer progression, our study will provide essential insights on the potential biological functions of H_2S.

EXPERIMENTAL SECTION

General Procedures

All reagents were used without further purification and purchased from commercial suppliers (unless otherwise specified). Ultrapure water was purified by the Milli-Q system with a resistivity of 18.25 MΩ·cm. The ^{1}H NMR (600 MHz) and ^{13}C NMR (151 MHz) spectra recorded at 25 °C using Bruker AV 600 MHz spectrometers were reported as parts per million (ppm) from tetramethylsilane as the internal standard. High-resolution mass spectra (HRMS) were determined by a Bruker MicroToF ESI LC-MS System in the positive-ion mode. HPLC (Agilent Technologies, USA) was conducted. Purities of new compounds 4, 5, 6, and 7 reached at least >95% purity by HPLC (Figures S21, S25, S29, and S33). FBS, RPMI 1640 medium, and other cell culture reagents were purchased from Gibco (Thermo Fisher Scientific, CA). UV−vis absorption spectra were recorded on a ThermoFisher Evolution 220 UV−vis spectrophotometer in 1 cm path-length quartz cells.

Preparation of Various Analyses. Various RSS or RONS were prepared according to the reported literature.[20] The testing solutions of $NaHSO_3$, Na_2SO_3, $Na_2S_2O_3$, NaSH, Vitamin C, Lys, Glu, GSH, and Cys were prepared by dissolving or diluting each of them in ultrapure water. ClO^- was prepared by dilution of commercial NaClO solution in ultrapure water, and the concentration was determined by measuring the absorbance at 209 nm. H_2O_2 was prepared by dilution of the commercial H_2O_2 solution, and the concentration was determined by measuring the absorbance at 240 nm. •OH was freshly generated by the Fenton reaction from ferrous ammonium sulfate and H_2O_2. $O_2^{\cdot-}$ was obtained by dissolving KO_2 in DMSO to make a 2 mM stock solution. NO was produced by slowly adding 4 M sulfuric acid to sodium nitrite solids, and the NO gas was purified before use by passing it through a NaOH solution to eliminate NO_2. All test solutions in the presence of nanoluciferase (Nluc) (0.5 μg/mL or 0.5 ng/mL) were allowed to stand for 20 min for measurement after being treated with RSS and other biomolecules.

Cell Culture. The 786-O-Nluc cells were maintained in an RPMI 1640 medium with 10% FBS and 1% antibiotic (penicillin-streptomycin) at 37 °C in a humidified incubator with 5% CO_2. The medium was changed every 24−48 h. The cells were subcultured at 90% confluence with 0.25% trypsin (w/v) every 2−3 days. Luciferase activities were determined using a multimode microplate reader (Infinite 200 PRO, Tecan). Total bioluminescent intensity counts are integrated over wavelengths from 400 to 800 nm, and the exposure time is 1000 ms.

Mice Model. NU/J female mice (6 weeks old) were purchased from Jackson Laboratory. All mouse protocols were in accordance with NIH guidelines and were approved by the Institutional Animal Care and Use Committee of Rice University. Animals were imaged using an IVIS Lumina II (Advanced Molecular Vision), following the recommended procedures and manufacturer's settings. To generate tumor xenografts in mice, the 786-O-Nluc cells (1×10^7) were implanted subcutaneously under the left flank region of each 7-week-old female nude mouse.

Imaging of Endogenous H_2S in 786-O-Nluc Xenograft Nude Mice. During the experiment, the nude mice were anesthetized with isoflurane. For monitoring the tumor growth, on the 3rd, 8th, and 12th days, QTZ (1 mM, 100 μL) was intravenously (retro-orbital (R.O.)) injected into four nude mice. For endogenous H_2S detection, QTZ-N_3 (1 mM, 100 μL) was intravenously (R.O.) injected into four nude mice on the 7th, 14th, and 30th days. On the 9th and 31st days, QTZ-Control (1 mM, 100 μL) was intravenously (R.O.) injected into nude mice. As the experiments with inhibitors, on the 31st day, 50 μL of AOAA (2 mM), PAG (2 mM), and $ZnCl_2$ (2 mM) was intratumorally injected into the mice. On the 8th day, 50 μL of BSO (2 mM) and PAG (2 mM) were intratumorally injected into the mice. Bioluminescence intensity was then measured for 300 s using the IVIS Imager. For the inhibition ratio, it can be calculated using the following formula:

$$\text{Inhibition ratio} = \frac{BL_{\text{before treatment}} - BL_{\text{after treatment}}}{BL_{\text{before treatment}}} \times 100\%$$

where $BL_{\text{before treatment}}$ is the luminescence intensity of the control mice (without inhibitor) and $BL_{\text{before treatment}}$ is the luminescence intensity of the mice with inhibitor treatment.

ASSOCIATED CONTENT

Supporting Information

The Supporting Information is available free of charge at https://pubs.acs.org/doi/10.1021/acsbiomedchemau.4c00102.

Other experimental details; photoluminescent properties of QTZ-DNP, QTZ-NBD, and QTZ-N_3; reaction mechanism between QTZ-N_3 and H_2S; other details

https://doi.org/10.1021/acsbiomedchemau.4c00102
ACS Bio Med Chem Au 2025, 5, 175−183

about cell experiments and animal experiments; and synthesis, NMR, HRMS, and HPLC data (PDF)

AUTHOR INFORMATION

Corresponding Author

Han Xiao − *Department of Chemistry, SynthX Center, Department of Biosciences, and Department of Bioengineering, Rice University, Houston, Texas 77005, United States;* orcid.org/0000-0002-4311-971X; Email: han.xiao@rice.edu

Authors

Kang Lu − *Department of Chemistry, Rice University, Houston, Texas 77005, United States*

Yixian Wang − *Department of Chemistry, Rice University, Houston, Texas 77005, United States;* orcid.org/0009-0004-3093-6835

Chenhang Wang − *Department of Chemistry, Rice University, Houston, Texas 77005, United States*

Rui Liu − *Department of Chemistry, Rice University, Houston, Texas 77005, United States*

Kaiqiang Yang − *Department of Chemistry, Rice University, Houston, Texas 77005, United States*

Xuanchenye Zhang − *Department of Chemistry, Rice University, Houston, Texas 77005, United States*

Complete contact information is available at: https://pubs.acs.org/10.1021/acsbiomedchemau.4c00102

Author Contributions

[⊥]K.L. and Y.W. contributed equally to this work. CRediT: **Kang Lu** conceptualization, data curation, formal analysis, investigation, methodology, validation, writing - original draft, writing - review & editing; **Yixian Wang** conceptualization, methodology, writing - original draft, writing - review & editing; **Chenhang Wang** conceptualization, investigation, writing - original draft, writing - review & editing; **Rui Liu** data curation, investigation; **Kaiqiang Yang** data curation, formal analysis, investigation; **Xuanchenye Zhang** data curation, formal analysis; **Han Xiao** conceptualization, funding acquisition, project administration, resources, supervision, writing - original draft, writing - review & editing.

Notes

The authors declare no competing financial interest.

ACKNOWLEDGMENTS

This work was supported by the Cancer Prevention Research Institute of Texas (CPRIT RR170014 to H.X.), NIH (R01-CA277838, R35-GM133706, R21-CA255894, and R01-AI165079 to H.X.), the Robert A. Welch Foundation (C-1970 to H.X.), the US Department of Defense (HT9425-23-1-0494 and W81XWH-21-1-0789 to H.X.), the John S. Dunn Foundation Collaborative Research Award (to H.X.), and the Hamill Innovation Award (to H.X.). H.X. is a Cancer Prevention & Research Institute of Texas (CPRIT) scholar in cancer research.

REFERENCES

(1) Szabo, C. Gasotransmitters in Cancer: From Pathophysiology to Experimental Therapy. *Nat. Rev. Drug Discov* **2016**, *15* (3), 185−203.

(2) Szabó, C. Hydrogen Sulphide and Its Therapeutic Potential. *Nat. Rev. Drug Discov* **2007**, *6* (11), 917−935.

(3) Liu, H.; Xue, S. Interplay between Hydrogen Sulfide and Other Signaling Molecules in the Regulation of Guard Cell Signaling and Abiotic/Biotic Stress Response. *Plant Communications* **2021**, *2* (3), No. 100179.

(4) Barresi, E.; Nesi, G.; Citi, V.; Piragine, E.; Piano, I.; Taliani, S.; Da Settimo, F.; Rapposelli, S.; Testai, L.; Breschi, M. C.; Gargini, C.; Calderone, V.; Martelli, A. Iminothioethers as Hydrogen Sulfide Donors: From the Gasotransmitter Release to the Vascular Effects. *J. Med. Chem.* **2017**, *60* (17), 7512−7523.

(5) Szabo, C.; Papapetropoulos, A. International Union of Basic and Clinical Pharmacology. CII: Pharmacological Modulation of H_2S Levels: H_2S Donors and H_2S Biosynthesis Inhibitors. *Pharmacol Rev.* **2017**, *69* (4), 497−564.

(6) Wang, D.; Yang, H.; Zhang, Y.; Hu, R.; Hu, D.; Wang, Q.; Liu, Y.; Liu, M.; Meng, Z.; Zhou, W.; Song, W. Inhibition of Cystathionine *β*-Synthase Promotes Apoptosis and Reduces Cell Proliferation in Chronic Myeloid Leukemia. *Sig. Transduct Target Ther.* **2021**, *6* (1), 52.

(7) Cirino, G.; Szabo, C.; Papapetropoulos, A. Physiological Roles of Hydrogen Sulfide in Mammalian Cells, Tissues, and Organs. *Physiol. Rev.* **2023**, *103* (1), 31−276.

(8) Cao, X.; Bian, J.-S. The Role of Hydrogen Sulfide in Renal System. *Front. Pharmacol.* **2016**, *7*, 385.

(9) Wallace, J. L.; Wang, R. Hydrogen Sulfide-Based Therapeutics: Exploiting a Unique but Ubiquitous Gasotransmitter. *Nat. Rev. Drug Discov* **2015**, *14* (5), 329−345.

(10) Sung, H.; Ferlay, J.; Siegel, R. L.; Laversanne, M.; Soerjomataram, I.; Jemal, A.; Bray, F. Global Cancer Statistics 2020: GLOBOCAN Estimates of Incidence and Mortality Worldwide for 36 Cancers in 185 Countries. *CA: A Cancer Journal for Clinicians* **2021**, *71* (3), 209−249.

(11) Moch, H.; Cubilla, A. L.; Humphrey, P. A.; Reuter, V. E.; Ulbright, T. M. The 2016 WHO Classification of Tumours of the Urinary System and Male Genital Organs—Part A: Renal, Penile, and Testicular Tumours. *European Urology* **2016**, *70* (1), 93−105.

(12) Hora, M.; Hes, O.; Reischig, T.; Ürge, T.; Klečka, J.; Ferda, J.; Michal, M.; Eret, V. Tumours in End-Stage Kidney. *Transplant. Proc.* **2008**, *40* (10), 3354−3358.

(13) Naro, Y.; Ankenbruck, N.; Thomas, M.; Tivon, Y.; Connelly, C. M.; Gardner, L.; Deiters, A. Small Molecule Inhibition of MicroRNA miR-21 Rescues Chemosensitivity of Renal-Cell Carcinoma to Topotecan. *J. Med. Chem.* **2018**, *61* (14), 5900−5909.

(14) Jiménez, D.; Martínez-Máñez, R.; Sancenón, F.; Ros-Lis, J. V.; Benito, A.; Soto, J. A New Chromo-Chemodosimeter Selective for Sulfide Anion. *J. Am. Chem. Soc.* **2003**, *125* (30), 9000−9001.

(15) Djokic, M. R.; Ristic, N. D.; Olahova, N.; Marin, G. B.; Van Geem, K. M. Quantitative On-Line Analysis of Sulfur Compounds in Complex Hydrocarbon Matrices. *Journal of Chromatography A* **2017**, *1509*, 102−113.

(16) Hall, J. R.; Schoenfisch, M. H. Direct Electrochemical Sensing of Hydrogen Sulfide without Sulfur Poisoning. *Anal. Chem.* **2018**, *90* (8), 5194−5200.

(17) Moon, C. H.; Zhang, M.; Myung, N. V.; Haberer, E. D. Highly Sensitive Hydrogen Sulfide (H_2S) Gas Sensors from Viral-Templated Nanocrystalline Gold Nanowires. *Nanotechnology* **2014**, *25* (13), No. 135205.

(18) Gao, M.; Yu, F.; Lv, C.; Choo, J.; Chen, L. Fluorescent Chemical Probes for Accurate Tumor Diagnosis and Targeting Therapy. *Chem. Soc. Rev.* **2017**, *46* (8), 2237−2271.

(19) Ma, J.; Sun, R.; Xia, K.; Xia, Q.; Liu, Y.; Zhang, X. Design and Application of Fluorescent Probes to Detect Cellular Physical Microenvironments. *Chem. Rev.* **2024**, *124* (4), 1738−1861.

(20) Yu, J.; Xu, J.; Ma, S.; Wang, C.; Miao, Q.; Wang, L.; Chen, G. Visible Tracking of Small Molecules of Gases with Fluorescent Donors. *Chemical & Biomedical Imaging* **2024**, *2* (6), 401−412.

(21) Sasakura, K.; Hanaoka, K.; Shibuya, N.; Mikami, Y.; Kimura, Y.; Komatsu, T.; Ueno, T.; Terai, T.; Kimura, H.; Nagano, T. Development of a Highly Selective Fluorescence Probe for Hydrogen Sulfide. *J. Am. Chem. Soc.* **2011**, *133* (45), 18003−18005.

(22) Zhang, K.; Zhang, J.; Xi, Z.; Li, L.-Y.; Gu, X.; Zhang, Q.-Z.; Yi, L. A New H_2S-Specific near-Infrared Fluorescence-Enhanced Probe That Can Visualize the H_2S Level in Colorectal Cancer Cells in Mice. *Chem. Sci.* **2017**, *8* (4), 2776−2781.
(23) Wu, L.; Sun, Y.; Sugimoto, K.; Luo, Z.; Ishigaki, Y.; Pu, K.; Suzuki, T.; Chen, H.-Y.; Ye, D. Engineering of Electrochromic Materials as Activatable Probes for Molecular Imaging and Photodynamic Therapy. *J. Am. Chem. Soc.* **2018**, *140* (47), 16340−16352.
(24) Zhang, Y.; Fang, J.; Ye, S.; Zhao, Y.; Wang, A.; Mao, Q.; Cui, C.; Feng, Y.; Li, J.; Li, S.; Zhang, M.; Shi, H. A Hydrogen Sulphide-Responsive and Depleting Nanoplatform for Cancer Photodynamic Therapy. *Nat. Commun.* **2022**, *13* (1), 1685.
(25) Wu, L.; Zeng, W.; Feng, L.; Hu, Y.; Sun, Y.; Yan, Y.; Chen, H.-Y.; Ye, D. An Activatable Ratiometric Near-Infrared Fluorescent Probe for Hydrogen Sulfide Imaging in Vivo. *Sci. China Chem.* **2020**, *63* (5), 741−750.
(26) Syed, A. J.; Anderson, J. C. Applications of Bioluminescence in Biotechnology and Beyond. *Chem. Soc. Rev.* **2021**, *50* (9), 5668−5705.
(27) Feng, P.; Zhang, H.; Deng, Q.; Liu, W.; Yang, L.; Li, G.; Chen, G.; Du, L.; Ke, B.; Li, M. Real-Time Bioluminescence Imaging of Nitroreductase in Mouse Model. *Anal. Chem.* **2016**, *88* (11), 5610−5614.
(28) Mostafa, I. M.; Abdussalam, A.; Zholudov, Y. T.; Snizhko, D. V.; Zhang, W.; Hosseini, M.; Guan, Y.; Xu, G. Recent Applications and Future Perspectives of Chemiluminescent and Bioluminescent Imaging Technologies. *Chemical & Biomedical Imaging* **2023**, *1* (4), 297−314.
(29) Zheng, M.; Huang, H.; Zhou, M.; Wang, Y.; Zhang, Y.; Ye, D.; Chen, H.-Y. Cysteine-Mediated Intracellular Building of Luciferin to Enhance Probe Retention and Fluorescence Turn-On. *Chemistry−A. European Journal* **2015**, *21* (29), 10506−10512.
(30) Ke, B.; Wu, W.; Wei, L.; Wu, F.; Chen, G.; He, G.; Li, M. Cell and in Vivo Imaging of Fluoride Ion with Highly Selective Bioluminescent Probes. *Anal. Chem.* **2015**, *87* (18), 9110−9113.
(31) Wu, W.; Li, J.; Chen, L.; Ma, Z.; Zhang, W.; Liu, Z.; Cheng, Y.; Du, L.; Li, M. Bioluminescent Probe for Hydrogen Peroxide Imaging in Vitro and in Vivo. *Anal. Chem.* **2014**, *86* (19), 9800−9806.
(32) Haris, U.; Kagalwala, H. N.; Kim, Y. L.; Lippert, A. R. Seeking Illumination: The Path to Chemiluminescent 1,2-Dioxetanes for Quantitative Measurements and In Vivo Imaging. *Acc. Chem. Res.* **2021**, *54* (13), 2844−2857.
(33) Ke, B.; Wu, W.; Liu, W.; Liang, H.; Gong, D.; Hu, X.; Li, M. Bioluminescence Probe for Detecting Hydrogen Sulfide in Vivo. *Anal. Chem.* **2016**, *88* (1), 592−595.
(34) Li, X.; Wang, A.; Wang, J.; Lu, J. Efficient Strategy for the Synthesis and Modification of 2-Hydroxyethylluciferin for Highly Sensitive Bioluminescence Imaging of Endogenous Hydrogen Sulfide in Cancer Cells and Nude Mice. *Anal. Chem.* **2019**, *91* (24), 15703−15708.
(35) Tian, X.; Li, Z.; Lau, C.; Lu, J. Visualization of in Vivo Hydrogen Sulfide Production by a Bioluminescence Probe in Cancer Cells and Nude Mice. *Anal. Chem.* **2015**, *87* (22), 11325−11331.
(36) Jiang, T.; Yang, X.; Yang, X.; Yuan, M.; Zhang, T.; Zhang, H.; Li, M. Novel Bioluminescent Coelenterazine Derivatives with Imidazopyrazinone C-6 Extended Substitution for Renilla Luciferase. *Org. Biomol. Chem.* **2016**, *14* (23), 5272−5281.
(37) Xiong, Y.; Zhang, Y.; Li, Z.; Reza, M. S.; Li, X.; Tian, X.; Ai, H. Engineered Amber-Emitting Nano Luciferase and Its Use for Immunobioluminescence Imaging In Vivo. *J. Am. Chem. Soc.* **2022**, *144* (31), 14101−14111.
(38) Hall, M. P.; Unch, J.; Binkowski, B. F.; Valley, M. P.; Butler, B. L.; Wood, M. G.; Otto, P.; Zimmerman, K.; Vidugiris, G.; Machleidt, T.; Robers, M. B.; Benink, H. A.; Eggers, C. T.; Slater, M. R.; Meisenheimer, P. L.; Klaubert, D. H.; Fan, F.; Encell, L. P.; Wood, K. V. Engineered Luciferase Reporter from a Deep Sea Shrimp Utilizing a Novel Imidazopyrazinone Substrate. *ACS Chem. Biol.* **2012**, *7* (11), 1848−1857.
(39) Mizui, Y.; Eguchi, M.; Tanaka, M.; Ikeda, Y.; Yoshimura, H.; Ozawa, T.; Citterio, D.; Hiruta, Y. Long-Term Single Cell Bioluminescence Imaging with C-3 Position Protected Coelenterazine Analogues. *Org. Biomol. Chem.* **2021**, *19* (3), 579−586.
(40) Lindberg, E.; Mizukami, S.; Ibata, K.; Miyawaki, A.; Kikuchi, K. Development of Luminescent Coelenterazine Derivatives Activatable by β-Galactosidase for Monitoring Dual Gene Expression. *Chemistry−A. European Journal* **2013**, *19* (44), 14970−14976.
(41) Orioka, M.; Eguchi, M.; Mizui, Y.; Ikeda, Y.; Sakama, A.; Li, Q.; Yoshimura, H.; Ozawa, T.; Citterio, D.; Hiruta, Y. A Series of Furimazine Derivatives for Sustained Live-Cell Bioluminescence Imaging and Application to the Monitoring of Myogenesis at the Single-Cell Level. *Bioconjugate Chem.* **2022**, *33* (3), 496−504.
(42) Lin, V. S.; Chen, W.; Xian, M.; Chang, C. J. Chemical Probes for Molecular Imaging and Detection of Hydrogen Sulfide and Reactive Sulfur Species in Biological Systems. *Chem. Soc. Rev.* **2015**, *44* (14), 4596−4618.
(43) Yu, F.; Han, X.; Chen, L. Fluorescent Probes for Hydrogen Sulfide Detection and Bioimaging. *Chem. Commun.* **2014**, *50* (82), 12234−12249.
(44) Fosnacht, K. G.; Pluth, M. D. Activity-Based Fluorescent Probes for Hydrogen Sulfide and Related Reactive Sulfur Species. *Chem. Rev.* **2024**, *124* (7), 4124−4257.
(45) Jiang, C.; Huang, H.; Kang, X.; Yang, L.; Xi, Z.; Sun, H.; Pluth, M. D.; Yi, L. NBD-Based Synthetic Probes for Sensing Small Molecules and Proteins: Design, Sensing Mechanisms and Biological Applications. *Chem. Soc. Rev.* **2021**, *50* (13), 7436−7495.
(46) Furne, J.; Saeed, A.; Levitt, M. D. Whole Tissue Hydrogen Sulfide Concentrations Are Orders of Magnitude Lower than Presently Accepted Values. *American Journal of Physiology-Regulatory, Integrative and Comparative Physiology* **2008**, *295* (5), R1479−R1485.
(47) Powell, C. R.; Dillon, K. M.; Matson, J. B. A Review of Hydrogen Sulfide (H_2S) Donors: Chemistry and Potential Therapeutic Applications. *Biochem. Pharmacol.* **2018**, *149*, 110−123.
(48) Amrolia, P.; Sullivan, S. G.; Stern, A.; Munday, R. Toxicity of Aromatic Thiols in the Human Red Blood Cell. *Journal of Applied Toxicology* **1989**, *9* (2), 113−118.
(49) Juneja, T. R.; Gupta, R. L.; Samanta, S. Activation of Monocrotaline, Fulvine and Their Derivatives to Toxic Pyrroles by Some Thiols. *Toxicol. Lett.* **1984**, *21* (2), 185−189.
(50) Montoya, L. A.; Pearce, T. F.; Hansen, R. J.; Zakharov, L. N.; Pluth, M. D. Development of Selective Colorimetric Probes for Hydrogen Sulfide Based on Nucleophilic Aromatic Substitution. *J. Org. Chem.* **2013**, *78* (13), 6550−6557.
(51) Henthorn, H. A.; Pluth, M. D. Mechanistic Insights into the H_2S-Mediated Reduction of Aryl Azides Commonly Used in H_2S Detection. *J. Am. Chem. Soc.* **2015**, *137* (48), 15330−15336.
(52) Xu, M.; Wang, Y.; Zhou, L.-N.; Xu, L.; Jin, Z.; Yang, D.; Chen, M.; Zhu, J. The Therapeutic Value of SC66 in Human Renal Cell Carcinoma Cells. *Cell Death Dis.* **2020**, *11* (5), 353.
(53) Sakurai, T.; Qu, W.; Sakurai, M. H.; Waalkes, M. P. A Major Human Arsenic Metabolite, Dimethylarsinic Acid, Requires Reduced Glutathione To Induce Apoptosis. *Chem. Res. Toxicol.* **2002**, *15* (5), 629−637.
(54) Abeles, R. H.; Walsh, C. T. Acetylenic Enzyme Inactivators. Inactivation of.Gamma.-Cystathionase, in Vitro and in Vivo by Propargylglycine. *J. Am. Chem. Soc.* **1973**, *95* (18), 6124−6125.
(55) Asimakopoulou, A.; Panopoulos, P.; Chasapis, C. T.; Coletta, C.; Zhou, Z.; Cirino, G.; Giannis, A.; Szabo, C.; Spyroulias, G. A.; Papapetropoulos, A. Selectivity of Commonly Used Pharmacological Inhibitors for Cystathionine β Synthase (CBS) and Cystathionine γ Lyase (CSE). *Br. J. Pharmacol.* **2013**, *169* (4), 922−932.
(56) Dong, Z.; Feng, L.; Chao, Y.; Hao, Y.; Chen, M.; Gong, F.; Han, X.; Zhang, R.; Cheng, L.; Liu, Z. Amplification of Tumor Oxidative Stresses with Liposomal Fenton Catalyst and Glutathione Inhibitor for Enhanced Cancer Chemotherapy and Radiotherapy. *Nano Lett.* **2019**, *19*, 805−815.

https://doi.org/10.1021/acsbiomedchemau.4c00102
ACS Bio Med Chem Au 2025, 5, 175−183